Structure and Properties of $(NEt_4)[Mo^VO(\alpha,2\text{-toluenedithiolato})_2]$. Distorted Tetragonal-Pyramidal $MoOS_4$ Core

Norikazu UEYAMA, Naoto YOSHINAGA, Atsushi KAJIWARA, Akira NAKAMURA,* and Masami KUSUNOKI†
Department of Macromolecular Science, Faculty of Science, Osaka University, Toyonaka, Osaka 560
†Institute for Protein Research, Osaka University, Suita, Osaka 565
(Received November 13, 1990)

An oxomolybdenum(V) complex with two chelating ligands of alkane- and arenethiolate parts, $(NEt_4)[Mo^VO(\alpha,2\text{-toluenedithiolato})_2]$, was prepared and characterized by visible, ESR, IR, and Raman spectroscopies. Four distinct ligand-to-metal charge transfer absorption bands were observed in visible region. The complex crystallizes in the space group $P2_1$ with a=9.535(2), b=16.582(9), c=8.085(1) Å, β=90.757(4)°, V=1278.3(8) Å^3, Z=2, and d_{calcd}=1.431 g cm^{-3}. The structure was solved and refinement based on 2102 reflections converged at R=0.089 and R_w=0.100. The complex takes an apical oxo and trans bis(α,2-toluenedithiolato) structure with a distorted $MoOS_4$ core from a tetragonal-pyramidal geometry.

The molybdenum center of sulfite oxidase has been considered to be bound to a bidentate dithiolene ligand connecting pterin and phosphate groups.[1,2] Recent EXAFS and ESR results indicate that the molybdenum center has one or more thiolate ligands besides the dithiolene ligand.[3,4] A $(Mo^VO)^{3+}$ complex having an unsymmetrical chelating dithiolato ligand has become of interest because tetrapeptide, Cys–X–Y–Cys (X,Y=amino acid residues), has a possibility to serve as an unsymmetrical dithiolate to activate $(Mo^VO)^{3+}$ ion.[5]

A simple model complex, $[Mo^VO(SPh)_4]^-$,[6] has been studied in detail. Some monooxomolybdenum(V) complexes having symmetrical dithiolate chelates have been reported as the precursor model complexes for the resting species of the active site of molybdoenzyme, e.g. $(Mo^VO(SCH_2CH_2S)_2]^-$,[7] $[Mo^VO(bdt)_2]^-$ (bdt=1,2-benzenedithiolato).[8] Relation between the number of thiolate ligands and the ESR parameter in $(MoOL_{4-x}L'_x)^-$ has been established.[9–11] Monooxomolybdenum(V) complexes have been systematically studied using a tridentate chelating ligand, e.g. hydrotris(3,5-dimethyl-1-pyrazolyl)borate.[12]

Complexation of two dithiolene type ligands and two alkanethiolates to $(MoO)^{3+}$ ion in unsymmetrical dithiolate, α,2-toluenedithiolate, seems to form an appropriate model complex for the active center of sulfite oxidase.

Experimental

All procedures were performed in argon atmosphere by the Schlenk technique. All solvents were dried and distilled under argon gas before use.

$(NEt_4)[Mo^VO(SPh)_4]$ was prepared by the reported method.[6] α,2-Toluenedithiol was synthesized by standard literature methods.[13]

Synthesis of (NEt_4) $[Mo^VO(\alpha\text{-tdt})_2]$ (α-tdt=α,2-toluenedithiolato) (1). The titled complex was synthesized by the following two methods. The crystals for the X-ray analysis were obtained by the method a.

a) From $(NEt_4)[MoO(SPh)_4]$ with Ligand Exchange Method. To a DMF solution (5 ml) of 35.7 mg (0.04 mmol) of $(NEt_4)[Mo^VO(SPh)]$ was added 0.017 ml (0.09 mmol) of α,2-toluenedithiol at room temperature. The solution was stirred overnight at room temperature and concentrated in vacuo to 0.5 ml volume. Addition of 10 ml of diethyl ether gave dark blue powder. The powder was collected with filtration and washed with 5 ml of diethyl ether. Recrystallization from DMF–diethyl ether gave dark blue microcrystals in 70% yield. Found: C, 47.13; H, 5.90; N, 2.75%. Calcd for $C_{22}H_{32}NOS_4Mo$: C, 47.98; H, 5.86; N, 2.54%.

b) From $MoOCl_3(thf)_2$. To an acetonitrile solution (10 ml) of 0.05 ml (0.3 mmol) of α,2-toluenedithiol and 0.09 ml (0.6 mmol) of triethylamine was added dropwise an acetonitrile solution of $MoOCl_3(thf)_2$ (58 mg, 0.16 mmol) at 0 °C. The solution turned dark green and was allowed to stand at room temperature for 5 h, before tetraethylammonium chloride (30 mg, 0.18 mmol) in methanol (6 ml) was added. After filtration the filtrate was concentrated in vacuo to 2 ml. Addition of methanol (30 ml) to the solution gave dark purple powder. The crude product was recrystallized from acetonitrile–methanol. Yield, 53%. Found: C, 47.17; H, 5.71; N, 2.61%. Calcd for $C_{22}H_{32}NOS_4Mo$: C, 47.98; H, 5.86; N, 2.55%.

Physical Measurements. Visible spectra were recorded in a solution of **1** or in a KBr disk on a JASCO Ubest-30 spectrophotometer. Infrared spectrum was taken in 400—200 cm^{-1} region as Nujol mulls and in 1000—400 cm^{-1} region as a KBr disc on a JASCO DS-402G spectrophotometer. Raman spectrum was obtained on a JASCO R-800 spectrophotometer equipped with an HTV-R649 photomultiplier. A powder sample in a capillary was irradiated with a 632.8 nm He–Ne laser excitation line. The frequency calibration of the spectrometer was carried out with indene as a standard. Electrochemical measurements were carried out using a Yanaco P-1100 instrument in acetonitrile solution that contained 0.1 M (1 M=1 mol dm^{-3}) tetrabutylammonium perchlorate as a supporting electrolyte. $E_{1/2}$ value, determined as $(E_{p,a}+E_{p,c})/2$, was referenced to the SCE electrode at room temperature and a value uncorrected with junction potential was obtained. ESR spectra in DMF–acetonitrile (1/4, v/v) were recorded on a JEOL JES-FE1X spectrometer at room temperature and at ca. 80 K.

X-Ray Structure and Determination. Single crystals of **1** grew from acetonitrile–ethanol. The crystal was sealed in a glass capillary under argon atmosphere for the X-ray measure-

Table 1. Crystallographic Data for $(NEt_4)[Mo^VO(\alpha\text{-tdt})_2]$ (1)

Chemical formula	$C_{22}H_{32}NOS_4Mo$
Fw	550.706
Cryst system	Monoclinic
a/Å	9.535(2)
b/Å	16.582(9)
c/Å	8.085(2)
β/deg	90.76(4)
V/Å^3	1278.3(8)
Z	2
Space group	$P2_1$
t/°C	20
d_{calcd}/g cm^{-3}	1.431
Radiation	Mo$K\alpha$
$2\theta_{max}$/deg	55.0
Scan type	θ–2θ
No. of reflections	Measured 3032
$I>3\sigma(I)$	Used 2102
R[a]	0.089
R_w[b]	0.100

a) $R=\sum||F_o|-|F_c||/\sum|F_o|$. b) $R_w=[\sum w(|F_o|-|F_c|)^2/\sum w|F_o|^2]^{1/2}$; $w=1/\sigma^2(|F_o|)$.

ment. The space group and approximate cell dimensions of the crystal were determined from oscillation and Weissenberg photographs. X-ray measurement was performed at 20 °C on a Rigaku AFC-4 diffractometer equipped with a Rotaflex rotating anode X-ray generator. The radiation used was Mo$K\alpha$ monochromatized with graphite (0.71069 Å). No absorption correction was made, although Lorentz and polarization corrections were applied. The basic crystallographic parameters for **1** are listed in Table 1. Unit cell dimensions were refined with 25 reflections. Three standard reflections were chosen and monitored with every 100 reflections and did not show any significant change. The positions of Mo, O, and S atoms were determined by the direct method using MULTAN 80. Subsequent Fourier synthesis based on the phases of Mo, O, and S atoms revealed the positions of the remaining non-hydrogen atoms. The final refinement was carried out using full-matrix least-squares techniques with non-hydrogen atoms. The y coordinate of the molybdenum atom was fixed in the refinement. The refinement with anisotropic thermal parameters is converged at R=0.089. Atom scattering factors and dispersion corrections were taken from the International Table.[14] The absolute configurations of the structure were determined from five Bijvoet pairs of reflections with large differences in $|F_o|$.

EHMO Calculations. In order to simplify extended Hückel MO calculations using an NEC PC-98 EHMO program obtained from Kodansha Sci. Co., $[Mo^VO(SCH{=}CH\text{-}CH_2S)_2]^-$ was employed instead of $[Mo^VO(\alpha\text{-tdt})_2]^-$ as a model complex. Two geometries were examined in the above model complex to evaluate the distortion of the Mo^VOS_4 core in $[Mo^VO(\alpha\text{-tdt})_2]$. One is a C_{4v} $MoOS_4$ core using the crystallographical parameters of $[Mo^VO(SPh)_4]^-$ reported in a literature.[6] Another is an idealized C_2 structure in $[Mo^VO(SCH{=}CH\text{-}CH_2S)_2]^-$ although $[Mo^VO(\alpha\text{-tdt})_2]^-$ as determined in this work has an approximate C_2 structure in Fig. 2. Mo–O, Mo–S, S–C, C–C, and C–H bond distances used are 1.680, 2.403, 1.760, 1.540, and 1.070 Å, respectively. A value, 109.9°, was employed for both Mo–S–C–H(CH_2) and Mo–S–C–H(CH=) torsion angles. A torsion angle, 120°, was adopted for S–C(H)=C–H and S–C(H_2)–C–H. The EHMO atomic parameters for Mo(V) were taken from a literature.[15]

Results and Discussion

Crystal Structure. The complex crystallizes in the space group $P2_1$ and the unit cell contains two $[Mo^VO(\alpha\text{-tdt})_2]^-$ anions and two NEt_4^+ cations. An ORTEP view of the $[Mo^VO(\alpha\text{-tdt})_2]^-$ ion is shown in Fig. 1. Only a trans isomer was obtained by the present synthetic method.

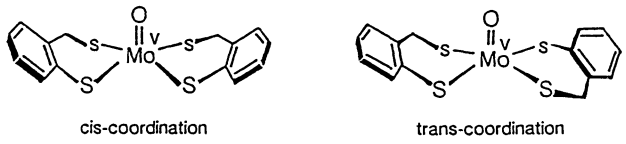

Table 2 lists the atomic coordinates of the non-hydrogen atoms and the estimated standard deviations. Selected bond distances and angles are listed in Table 3.[16] The coordination around the molybdenum atom is a distorted tetragonal-pyramidal geometry with an approximate C_2 symmetry, containing the one terminal oxo, the two alkanethiolato and the two arenethiolato ligands. The Mo=O distance is 1.688(18) Å which is in a range 1.64—1.72 Å observed for various Mo(V)=O

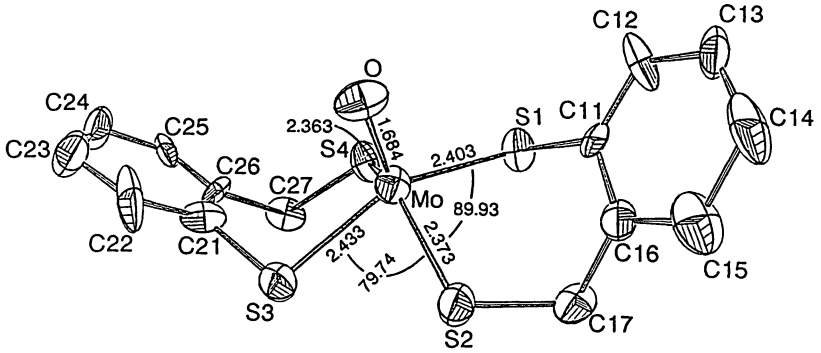

Fig. 1. ORTEP view of $(NEt_4)[Mo^VO(\alpha\text{-tdt})_2]$ (**1**) showing the atom-labeling scheme.

Table 2. Atomic Coordinates and Equivalent Isotropic Thermal Parameters for $(NEt_4)[Mo^VO(\alpha\text{-tdt})_2]$ (1)

Atom	x	y	z	B_{eqv}[a)]/Å^2
Mo	0.8719(2)	0.1620(0)	0.7103(3)	1.80(2)
S1	0.6901(7)	0.0621(4)	0.7326(8)	3.05(10)
S2	0.9214(6)	0.1159(4)	0.4400(8)	3.05(10)
S3	1.1189(7)	0.1969(5)	0.6938(8)	3.24(11)
S4	0.9104(6)	0.1144(5)	0.9830(8)	3.07(10)
O	0.7890(19)	0.2519(10)	0.7107(21)	1.95(32)
C11	0.5888(20)	0.0729(12)	0.5486(27)	2.05(33)
C12	0.4460(21)	0.0946(13)	0.5532(28)	2.96(41)
C13	0.3704(26)	0.0979(18)	0.4115(30)	3.22(49)
C14	0.4273(28)	0.0847(18)	0.2530(38)	4.08(56)
C15	0.5762(27)	0.0599(17)	0.2462(36)	2.91(53)
C16	0.6538(24)	0.0588(16)	0.3916(35)	3.18(45)
C17	0.7994(25)	0.0308(15)	0.3830(33)	3.25(42)
C21	1.1436(25)	0.2586(15)	0.8762(28)	3.33(41)
C22	1.1754(29)	0.3393(18)	0.8617(37)	4.50(56)
C23	1.1996(30)	0.3878(17)	0.9976(43)	3.91(57)
C24	1.1792(26)	0.3509(15)	1.1610(32)	3.38(49)
C25	1.1505(20)	0.2681(14)	1.1683(28)	3.39(35)
C26	1.1315(22)	0.2238(15)	1.0328(34)	3.41(42)
C27	1.0994(24)	0.1349(12)	1.0382(26)	2.85(38)
N	0.3227(19)	−0.1448(12)	0.7822(26)	3.50(36)
C31	0.1896(30)	−0.1555(17)	0.6724(41)	3.31(58)
C32	0.1589(39)	−0.0781(26)	0.5774(56)	3.81(104)
C33	0.3417(30)	−0.2281(15)	0.8744(36)	3.24(56)
C34	0.4664(29)	−0.2300(23)	1.0041(45)	4.20(66)
C35	0.4555(26)	−0.1254(18)	0.6822(34)	3.39(48)
C36	0.4911(41)	−0.1847(24)	0.5470(47)	4.87(96)
C37	0.3047(36)	−0.0772(19)	0.9075(43)	3.61(70)
C38	0.1758(37)	−0.0853(21)	1.0299(38)	4.06(68)

a) B_{eqv} is defined as the equivalent isotropic displacement parameter as $1/3[a^2a^{*2}B_{11}+b^2b^{*2}B_{22}+c^2c^{*2}B_{33}+2ab(\cos\gamma)a^*b^*B_{12}+2ac(\cos\beta)a^*c^*B_{13}+2bc(\cos\alpha)b^*c^*B_{23}]$.

Table 3. Selected Intramolecular Distances and Angles for $(NEt_4)[Mo^VO(\alpha\text{-tdt})_2]$ (1)[17]

	Bond distances	l/Å
Mo–O		1.688(18)
Mo–S(1)		2.406(7)
Mo–S(2)		2.368(7)
Mo–S(3)		2.431(7)
Mo–S(4)		2.366(7)
S(1)–C(11)		1.771(23)
S(2)–C(17)		1.881(27)
S(3)–C(21)		1.811(26)
S(4)–C(27)		1.881(24)
S(1)–S(2)		3.375(9)
S(2)–S(3)		3.075(10)
S(3)–S(4)		3.379(10)
S(4)–S(1)		3.025(9)
	Bond angles	θ/°
S(1)–Mo–O		105.34(64)
S(2)–Mo–O		112.92(64)
S(3)–Mo–O		104.53(64)
S(4)–Mo–O		110.92(64)
S(1)–Mo–S(2)		89.93(23)
S(2)–Mo–S(3)		79.74(23)
S(3)–Mo–S(4)		89.28(23)
S(4)–Mo–S(1)		78.75(23)
S(1)–Mo–S(3)		150.10(24)
S(2)–Mo–S(4)		136.15(23)

complexes. Two types of Mo–S bonds were found; longer ones (2.40(1) Å and 2.43(1) Å) for the molybdenum-arenethiolate and shorter ones (2.37(1) Å and 3.37(1) Å) for the molybdenum-alkanethiolate bonds. This trend is expected from the difference in the bond lengths between $[Mo^VO(SPh)_4]^-$ and $[Mo^VO(SCH_2CH_2S)_2]^-$.[6,7] The larger S pπ-donation of alkanethiolato ligand to $(MoO)^{3+}$ contributes to increase of the Mo–S bond order. Figure 2 shows the schematic drawing of the distortion in **1**. The two alkanethiolate Mo–S bonds give larger O–Mo–S bond angles (mean 112°) and a smaller trans S–Mo–S angle (136.2(3)°) while the two arenethiolate Mo–S bonds provide smaller O–Mo–S bond angles (mean 105°) and a larger trans S–Mo–S (150.1(3)°). The Mo^VOS_4 core

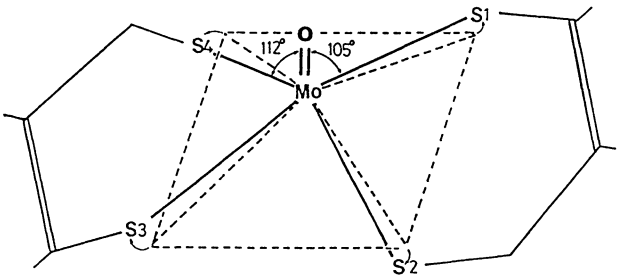

Fig. 2. Schematic drawing of the distortion of $(NEt_4)[Mo^VO(\alpha\text{-tdt})_2]$ (1).

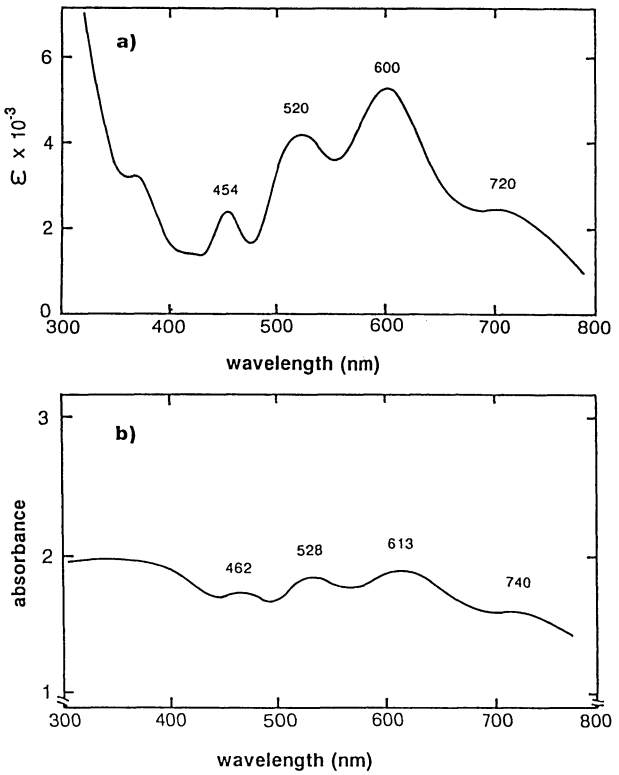

Fig. 3. Visible spectra of $(NEt_4)[Mo^VO(\alpha\text{-tdt})_2]$ (1) a) in acetonitrile solution and b) in the solid state (KBr matrix).

of $[Mo^{V}O(SPh)_4]^-$ was reported to have two O–Mo–S angles, 108.5(3)° and 111.2(3)°. Only one example for similar distortion has been reported for $[Mo^{V}O(SCH_2CH_2CH_2S)_2]^-$ which has two kinds of large trans S–Mo–S angle (149.9(1)° and small trans S–Mo–S angle (138.8(1)°).[17] The presence of two kinds of S–Mo–S bond angles is probably due to the large bite angle ca. 89° of α,2-toluenedithiolate. It is noticeable that the distortion of the $MoOS_4$ core in **1** is the largest among the known ones.

Properties of 1. Figures 3-a and 3-b shows the visible spectra of **1** in solution and in the solid KBr matrix, respectively. Four distinct absorption maxima were observed at 454 nm (ε, 2300 $mol^{-1}\,cm^{-1}$), 520 nm (4100), 600 nm (5200), and 720 nm (2300) in an acetonitrile solution. Four maxima at 462, 528, 613, and 740 nm were also obtained in the KBr matrix with the same ratio of the absorbance as shown in Fig. 3-b. The spectra of **1** indicate that only the trans isomer exists both in solutions and in the solid state as established by the crystallographic analysis. These intense absorption maxima (ε, 2300—5200 $mol^{-1}\,cm^{-1}$) could be assigned to ligand-to-metal charge-transfer (LMCT) bands. Actually, the broad absorption maxima due to LMCT in the visible region of approximate C_{4v} Mo(V)=O complexes, e.g. 602 nm (6400 $mol^{-1}\,cm^{-1}$ in acetonitrile) for $(NEt_4)[Mo^{V}O(SPh)_4]$, have been extensively studied by Ellis et al.[18] They have pointed out that the low energy d-d transition due to Mo(V)=O group is masked by the dominant LMCT bands. For example, only a weak absorption maximum has been reported at 670 nm with 20 $mol^{-1}\,cm^{-1}$ in this region for $[Mo^{V}OCl_4]^-$ in CH_2Cl_2.[19]

EHMO calculations were carried out to interpret the difference between the ideal square-pyramidal structure (four trans S–Mo–S angles are 140°) and the distorted structure (two trans S–Mo–S angles are 136° and 150°) in $[Mo^{V}O(SCH_2CH{=}CHS)_2]^-$. The distorted structure corresponds to that of **1** analyzed cystallographically. No significant difference was found in the energy levels of d-orbitals between them. This result suggests that the four distinct absorption maxima are ascribed not to d-d transition but to the ligand-to-metal charge transfer from two or more sulfur pπ orbitals to Mo(V) d_{xy} orbital as induced by the lower symmetry of α,2-toluenedithiolate. Figure 4 shows the IR and Raman spectra of **1** in solid state. The Raman and IR spectra in solid state showed a strong ν(Mo=O) mode at 940 and 938 cm^{-1}, respectively. An IR Mo=O band has been reported to appear in the same region at 929 cm^{-1} for $(NEt_4)[Mo^{V}O(SPh)_4]$.[6] The higher-wavenumber shift is ascribed to the less π-donor ability of arenethiolate ligand than alkanethiolate liagnd. Actually, the higher-wavenumber shift has been established in the case of the larger π-donor ability of the thiolate ligands in $[MoO(SR)_4]^-$ (SR=SPh, S-4-$CH_3C_6H_4$, S-4-ClC_6H_4, S-3-ClC_6H_4, S-4-FC_6H_4, S-2,6-$Cl_2C_6H_3$, and SC_6F_5).[18] Intense Raman bands at 444 and 352 cm^{-1} are tentatively assigned to ν(Mo–S). Strong IR bands observed at 385, 361, 344, and 302 cm^{-1} are associated with IR active ν(Mo–S) frequencies. The results reflect decrease in symmetry of **1**.

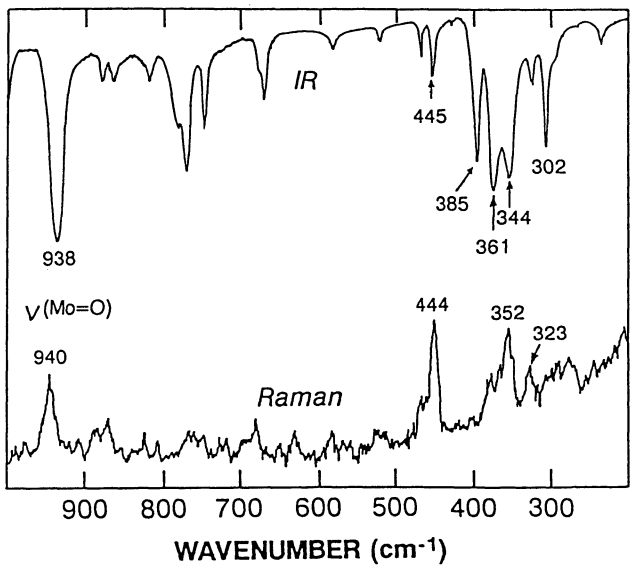

Fig. 4. IR and Raman spectra of $(NEt_4)[Mo^{V}O(\alpha\text{-}tdt)_2]$ (**1**) in solid state.

The electrochemical property of **1** was studied using cyclic voltammetry of a solution in 0.1 M $(n\text{-}Bu)_4NCl$–DMF. A reversible couple was observed at −0.73 V vs. SCE that corresponds to a one-electron reduction of the complex. An irreversible oxidation peak was given at +0.65 V due to the Mo(V)/Mo(VI) couple. The Mo(V)/Mo(IV) redox potential of **1** in DMF is expected to be higher compared with that of $(NEt_4)[Mo^{V}O(SPh)_4]$ (−0.75 V in acetonitrile) because of the larger electron donation from alkanethiolato to $(Mo^{V}O)$ ion than that of arenethiolato. The redox potential is found to become more positive by the electron-withdrawing character of the thiolate ligands as has been pointed for *p*-substituted benzenethiolate molybdenum(V) complexes by Ellis et al.[18] Therefore, **1** would be expected to exhibit a more negative redox potential due to the presence of two alkanethiolate ligands, but it shows a more positive one (−0.73 V vs. SCE in acetonitrile) than that (−0.77 V in acetonitrile) of $[Mo^{V}O(SPh)_4]^-$.[6] We examined the difference in SOMO orbital energies between the regular square-pyramidal and the distorted structures for the simple model complex, $[Mo^{V}O(SCH_2CH{=}CHS)_2]^-$, using EHMO calculations. The SOMO orbital energies for the regular structure and the distorted structure are −10.315 and −10.323 eV, respectively. The results can be explained by the ease of reduction of the distorted **1**. It is likely that this distortion induces the variation of O=Mo–S–C torsion angle accompanied with the change of π-interaction in Mo–S bond.

A DMF–CH_3CN solution (1 : 4) of **1** exhibited an axial ESR signals at room temperature and at ca. 80 K

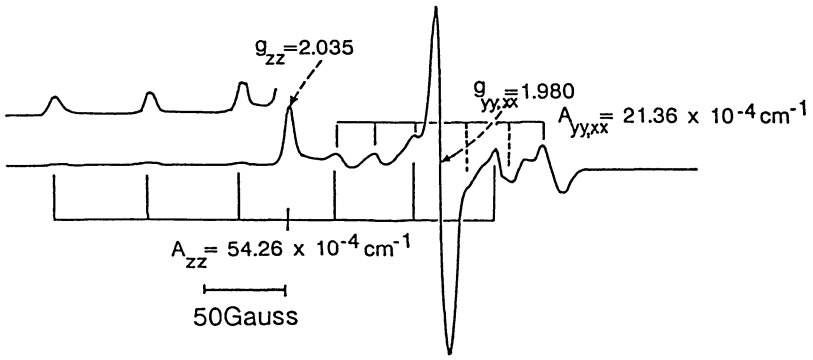

Fig. 5. ESR spectra of $(NEt_4)[Mo^VO(\alpha\text{-tdt})_2]$ (**1**) in DMF–acetonitrile freezing solution at ca. 80 K.

Table 4. ESR Parameters of $(NEt_4)[Mo^VO(\alpha\text{-tdt})_2]$ (**1**) and Various Related Mo(V) Thiolate Complexes

Complex	g_{zz}	g_{yy}	g_{xx}	A_{zz}	A_{yy}	A_{xx}	Ref
				$\times 10^4$ cm^{-1}			
$[MoO(SCH_2CH_2S)_2]^-$	2.012	1.997	1.975				11
$[MoO(bdt)_2]^-$	2.022	1.984	1.976	47.2			12
$[MoO(\alpha\text{-tdt})_2]^-$	2.035	1.980		54.3	21.3		This work
$[MoO(SPh)_4]^-$	2.017	1.979		52.3	22.3		10

Table 5. Influence of the $MoOS_4$ Core Distortion on Molybdenum(V) Ion MO Coefficients of the SOMO in $[Mo^VO(SCH_2CH{=}CHS)_2]^-$

Geometry	MO coefficients of SOMO in Mo(V) ion								
	s	p_x	p_y	p_z	$d_{x^2-y^2}$	d_{z^2}	d_{xy}	d_{xz}	d_{yz}
Regular $MoOS_4$ all O–Mo–S 110°	0.005	0.00	0.00	−0.023	−0.034	0.044	−0.937	0.00	0.00
Distorted $MoOS_4$ O–Mo–S1, O–Mo–S3=113° O–Mo–S2, O–Mo–S4=105°	0.004	0.00	0.00	−0.022	−0.049	0.044	−0.933	0.00	0.00

as shown in Fig. 5. The low-temperature ESR measurement for **1** provided g_{zz}=2.035 at ca. 80 K which is a relatively large value in the synthetic molybdenum(V) thiolate complexes. The ESR parameters are compared with those of various molybdenum(V) thiolate complexes in Table 4. The axial signals for **1** are obtained even in the distortion from a tetragonal-pyramidal to an approximate C_2 structure as revealed by the crystallographic analysis. In the various cases of monooxomolybdenum(V) complexes, g tensor has been determined to coincide with Mo=O direction, e.g. $[Mo^VOCl_4]^-$.[19] The large g_{zz} value should reflect the ligand field equatorial to the Mo=O bond axis because of spin-orbit coupling between Mo and sulfur. Furthermore, the low-energy charge-transfer transition also contributes to the observed g_{zz} value shift in addition to the above ligand field because the SOMO of Mo(V) calculated by the EHMO method shows the contribution from S $p\pi$-orbitals as described later. Therefore, the reported small value of g_{zz} for $[Mo^VO(SCH_2CH_2S)_2]^-$ is in conflict with the tendency of large electron-donating character of the alkanethiolato ligand.

Table 5 lists the MO coefficients of the SOMO in the simple model complex, $[Mo^VO(SCH_2CH{=}CHS)_2]^-$ for **1** to evaluate the influence of the distortion to the ESR signals of **1**. The EHMO calculations were carried out in two geometries which are regular and distorted. The difference between the SOMO electron densities for the two geometries by mixing p_z and d_{z^2} orbitals in the z direction is not so large that the distortion of the $MoOS_4$ core does not influence the MO electron density in SOMO contributing to the shift of the g_{zz} value. The results are coincident with a small change reported in the ESR signals between $[Mo^VOCl_4]^-$ and $[Mo^VOCl_5]^{2-}$.[19] Further study will be required to examine this trend on the ESR parameters.

We thank Professor Mikiharu Kamachi for the ESR measurement. We gratefully acknowledge partial support of this research by a Grant-in-Aid for Scientific Research on Priority Areas of "Macromolecular Com-

plexes" No63612093 from the Ministry of Education, Science and Culture.

References

1) R. C. Wahl and K. V. Rajagopalan, *J. Biol. Chem.*, **257**, 1354 (1982).
2) J. L. Johnson and K. V. Rajagopalan, *Proc. Natl. Acad. Sci. U.S.A.*, **79**, 6856 (1982).
3) S. P. Cramer, R. Wahl, and K. V. Rajagopalan, *J. Am. Chem. Soc.*, **103**, 7721 (1981).
4) R. C. Bray, *Adv. Enzymol. Relat. Areas Mol. Biol.*, **51**, 107 (1980).
5) N. Ueyama, N. Yoshinaga, A. Kajiwara, and A. Nakamura, *Chem. Lett.*, **1990**, 1781.
6) a) G. R. Hanson, A. A. Brunette, A. C. McDonell, K. S. Murray, and A. G. Wedd, *J. Am. Chem. Soc.*, **103**, 1953 (1981). b) I. W. Boyd, I. G. Dance, K. S. Murry, and A. G. Wedd, *Aust. J. Chem.*, **31**, 279 (1978).
7) S. R. Ellis, D. Collison, C. D. Garner, and W. Clegg, *J. Chem. Soc., Chem. Commun.*, **1986**, 1483.
8) S. Boyde, S. R. Ellis, C. D. Garner, and W. Clegg, *J. Chem. Soc., Chem. Commun.*, **1986**, 1541.
9) R. C. Bray, "Enzymes," 3rd ed, 1975, Vol. 12, p. 299.
10) J. T. Spence, M. Minelli, P. Kroneck, M. I. Scullane, and N. D. Chasteen, *J. Am. Chem. Soc.*, **100**, 8002 (1978).
11) M. I. Scullane, R. D. Tylor, M. Minelli, J. T. Spence, K. Yamanouchi, J. H. Enemark, and N. D. Chasteen, *Inorg. Chem.*, **18**, 3213 (1979).
12) C. G. Young, J. H. Enemark, D. Collison, and F. E. Mabbs, *Inorg. Chem.*, **26**, 2925 (1987).
13) a) E. Klingsberg and A. M. Schreiber, *J. Am. Chem. Soc.*, **84**, 2941 (1962). b) A. G. Hortmann, A. J. Aron, and A. K. Bhattacharya, *J. Org. Chem.*, **43**, 3374 (1978).
14) "International Tables for a X-Ray Crystallography," Kynoch, Birmingham, England (1974), Vol. IV, p. 99.
15) M. Kamata, K. Hirotsu, T. Higuchi, K. Tatsumi, R. Hoffmann, T. Yoshida, and S. Otsuka, *J. Am. Chem. Soc.*, **103**, 5772 (1981).
16) The table of anisotropic parameters of non-hydrogen atoms, the F_o-F_c table and the tables of bond distances and angles are deposited as Document No. 8953 at the Office of the Editor of Bull. Chem. Soc. Jpn.
17) P. T. Bishop, J. R. Dilworth, J. Hutchinson, and J. A. Zubieta, *J. Chem. Soc., Chem. Commun.*, **1982**, 1052.
18) S. R. Ellis, D. Collison, and C. D. Garner, *J. Chem. Soc., Dalton Trans.*, **1989**, 413.
19) C. D. Garner, L. H. Hill, F. E. Mabbs, D. L. McFadden, and A. T. McPhail, *J. Chem. Soc., Dalton Trans.*, **1977**, 853.